AIP Journal of Applied Physics

Reaction of the Si/Ta/Ti system: C40 TiSi 2 phase formation and in situ kinetics

F. La Via, F. Mammoliti, and M. G. Grimaldi

Citation: Journal of Applied Physics **91**, 633 (2002); doi: 10.1063/1.1421212
View online: http://dx.doi.org/10.1063/1.1421212
View Table of Contents: http://scitation.aip.org/content/aip/journal/jap/91/2?ver=pdfcov
Published by the AIP Publishing

Reaction of the Si/Ta/Ti system: C40 $TiSi_2$ phase formation and *in situ* kinetics

F. La Via[a)]
CNR-IMETEM, Stradale Primosole 50, 95121 Catania, Italy

F. Mammoliti and M. G. Grimaldi
INFM and Departimento di Fisica e Astronomia, Corso Italia 57, Catania, Italy

(Received 26 July 2001; accepted for publication 1 October 2001)

The effect of a thin Ta layer at the Si/Ti interface on the intermediate phase formation has been studied in detail by *in situ* sheet resistance, X-ray diffraction and transmission electron microscopy of partially reacted samples. When a Ta layer is deposited at the Si/Ti interface, a new intermediate phase has been detected, i.e., the hexagonal $TiSi_2$ C40. This phase grows on the C40 $TaSi_2$ that is formed at the interface with silicon. The activation energies of the C40 formation (1.9 ± 0.3 eV) and the C40–C54 phase transition (3.7 ± 0.5 eV) have been determined and compared to the activation energies for the C49 (1.7 ± 0.1 eV) formation and the C49–C54 (5.1 ± 0.9 eV) transition. Both the transformation kinetics and the film morphology are consistent with an increase of the nucleation density with respect to the C49–C54 transition. © *2002 American Institute of Physics.*
[DOI: 10.1063/1.1421212]

I. INTRODUCTION

$TiSi_2$ is widely used as a self-aligned silicide (salicide) for the metallization of gates, sources/drains, and local interconnects in ultralarge scale integration devices and circuits. In thin films, two crystalline phases appear, and the metastabile C49–$TiSi_2$ usually forms before the final C54–$TiSi_2$ phase.[1] The transformation from C49 to C54 phase becomes more difficult in submicron lines because of the low density[2] of nucleation sites. In recent papers,[3–5] it was shown that the presence of Mo, Ta, or Nb impurities at the metal–silicon interface lowers the formation temperature of the C54 phase with respect to pure Ti/Si bilayers. In a first attempt, this reduction was attributed to the suppression of the intermediate C49 phase.[6] Later measurements[7] by high resolution transmission electron microscopy (TEM) indicated the formation of a ternary compound (TiTa)Si_2 C40 at the Ti/Si interface that acts as a seed for the successive growth of the $TiSi_2$ C40 phase. The C54 phase transition starts to take place after the formation of the C40 phase. In a recent paper[8] it has been observed that the transition from the C40 to the C54 is nucleation limited. X-ray diffraction[9] (XRD) analysis clearly showed a large area C40 $TiSi_2$ layer grown on the C40 $TaSi_2$ and the experimentally determined lattice parameters of the phase agree quite well with those obtained by *ab initio* calculations.

In this article, we show that the formation of a pseudomorphic C40 $TiSi_2$ phase over the C40 $TaSi_2$ layer is responsible of the mentioned temperature reduction. This has been inferred from a detailed study of the phase sequence during the reaction of a Si/Ta/Ti system. The transformation kinetic has been monitored by *in situ* sheet resistance measurements, by *ex situ* TEM and Bragg–Bentano XRD. These measurements have been performed on different samples with different tantalum thickness at the Ti/Si interface and the behavior of the different kinetics has been discussed in detail.

II. EXPERIMENT

Samples were prepared in a ultrahigh vacuum chamber by sequential deposition of a 150 nm amorphous Si layer, different Ta layer thickness and 20 nm Ti on thermally oxidized 5 in. silicon wafers.

For the sake of comparison, we also prepared one sample without Ta, where the thickness of the Ti layer was maintained at 20 nm. Samples are designated as A, B, C (no tantalum, 1.9×10^{15} and 4.5×10^{15} atoms/cm^3 of Ta, respectively). *In situ* sheet resistance measurements were performed during the annealing in the temperature range between 600–675 °C at a pressure of 1×10^{-7} Torr. XRD measurements were carried out on a Bruker D5005 diffractometer operating in the Seeman–Bohlin grazing angle, (G-A) and Bragg–Brentano configuration. Measurements were performed using the Cu $K\alpha$ ($\lambda=0.154\,06$ nm) with the x-ray source accelerating voltage of 40 kV and 40 mA current. In G-A configuration, the x-ray beam was incident at 1° on the sample surface and the detector angle was incremented with an angular step of 0.1°. The film grain size determination was carried out by TEM in plan view configuration. The different phases were identified by selected area electron diffraction and dark field images.

III. RESULTS AND DISCUSSION

The *in situ* sheet resistance versus time curve, recorded during the annealing at 660 °C of the Si/Ti sample, and normalized to the starting value R_{s0} is reported in Fig. 1(a). The final temperature on the sample was reached by stabilizing the system at intermediate values before starting the mea-

a)Electronic mail: lavia@imetem.ct.cnr.it

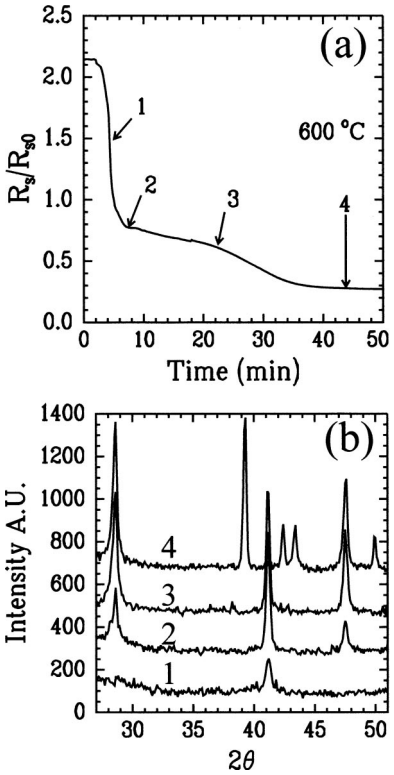

FIG. 1. (a) *In situ* sheet resistance of the Si/Ti sample. Four different samples were stopped at the annealing time indicated by the arrows. The G-A XRD spectra of the partially reacted samples are reported in (b).

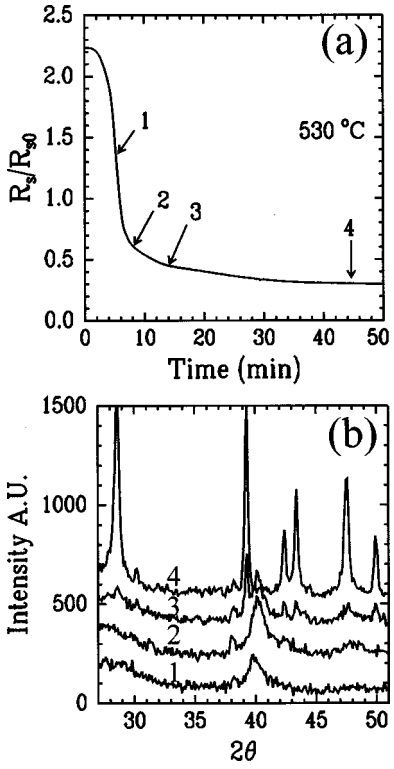

FIG. 2. (a) *In situ* sheet resistance of the Si/Ta/Ti sample. Four different samples were stopped at the annealing time indicated by the arrows. The G-A XRD spectra of the partially reacted samples are reported in (b).

sure. The initial sheet resistance at $t=0$ is due to the unreacted Ti film deposited on top of the amorphous Si layer. At the beginning of the annealing, the sheet resistance decreases with a high rate until it reaches a value of about 25 Ω/square [$R_s/R_{s0}=0.76$ in Fig. 1(a)] after ~5 min. During the successive ~20 min, the resistance decreases slowly and an almost flat region appears in the sheet resistance signal, then a fast decrease turns the value to the one of the stable phase, corresponding to ~10 Ω/square [$R_s/R_{s0}=0.27$ in Fig. 1(a)]. The resistivity at room temperature of partially reacted sample [labeled 2 in Fig. 1(a)] is 84 $\mu\Omega$ cm, while the final phase has a value of 15 $\mu\Omega$ cm, typical of the C54 phase. In order to characterize the transition, the annealing was stopped for *ex situ* characterization at different times (Fig. 1, see the arrows). The corresponding G-A XRD patterns are reported in Fig. 1(b). In this configuration, the planes that are parallel to the sample surface are not visible. The pattern of the sample annealed for 8 min (No. 1) exhibits a single peak at 41° that can be attributed to the C49(131) planes. The peak intensity is moderate since the reaction is not yet complete. The remaining Ti layer is textured along the (002) and (101) crystallographic directions, as detected by B–B XRD analyses (not shown). The diffraction pattern relative to the partially reacted samples 2 and 3 exhibits three peaks at 28.5°, 41°, 47.5°. These peaks are related to the diffractions of the Si(111), C49(131), and Si(220) planes, respectively, and become progressively more intense until the reaction is complete and titanium is totally transformed into C49 $TiSi_2$. Finally, the sample annealed for more than 40 min (No. 4) reaches the steady state R_s value and shows, besides the two peaks of the Si, four sharp peaks at 39°, 42.5°, 43.5°, and 50°. These peaks can be attributed to the C54(311), C54(040), C54(022), and C54(331) diffractions. Therefore, the first drop of the resistance versus time curve is due to the formation of the C49 phase, the second one to the formation of the C54 phase.

The *in situ* sheet resistance versus time curve of the sample B, which has 1.9×10^{15} atom/cm^3 of Ta at the Ti/Si interface is shown in Fig. 2(a). The annealing temperature of this sample was lowered to 600 °C in order to achieve transition time comparable to that of pure Ti/Si. Even in this case, there is an initial fast decrease followed by a more flat region and, at longer times, a final decrease to the steady state value of 10.6 Ω/square [$R_s/R_{s0}=0.30$ in Fig. 2(a)]. However, in the presence of Ta, the flat region (No. 2 →No. 3) is badly defined since it lasts for a relatively short time and the sheet resistance of the intermediate phase is about $0.55R_{s0}$, lower than that one of the sample without Ta ($R_s\sim0.7R_{s0}$). The resistivity at room temperature of the partially reacted sample [labeled 2 in Fig. 2(a)] is 44 $\mu\Omega$ cm, while that of the final phase is 15 $\mu\Omega$ cm, typical of the C54 phase, as in Si/Ti sample.

The G-A XRD patterns, relatives to the partially reacted silicides marked by the arrows in Fig. 2(a), are reported in Fig. 2(b). Sample Nos. 1 and 2 exhibit a single peak at 40° that can be attributed to the $TaSi_2$ $(2\bar{1}1)$. The intensity is weak because of the limited amount of Ta. At longer annealing times (No. 3), besides the $TaSi_2$ peak, there is a peak at 39° that can be attributed to the C54(311), although the reaction is not complete. At the steady state (No. 4), there are

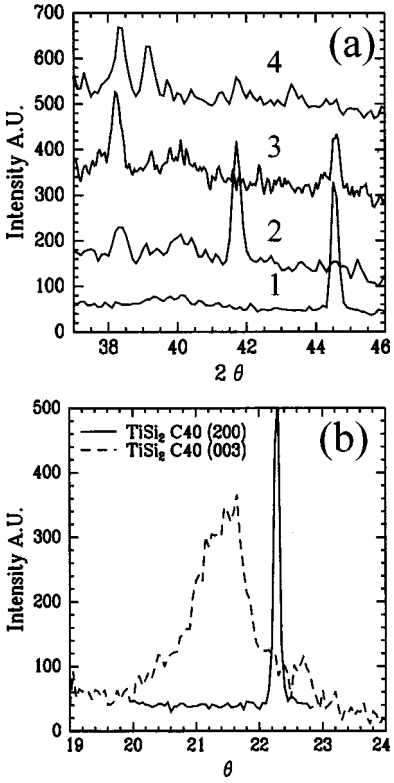

FIG. 3. (a) Bragg–Bentano XRD spectra of the Si/Ta/Ti sample partially reacted. The peaks of the C40 $TiSi_2$ are clearly visible at 38.3°, 41.7°, and 44.5° in the first three samples. The rocking curves relative to the C40 $TiSi_2$ (200) and C40 $TiSi_2$ (003) are reported in (b).

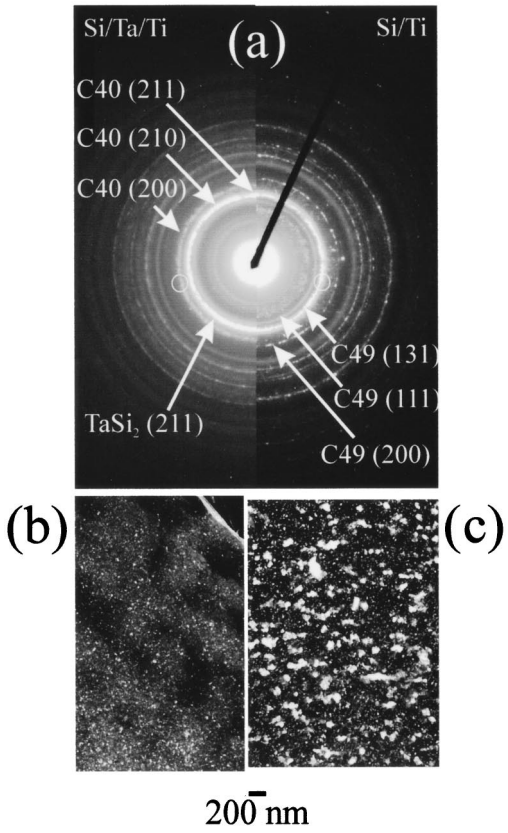

FIG. 4. (a) Transmission electron diffraction of the intermediate phases for the Si/Ta/Ti sample (left-hand side) and the Si/Ti sample (right-hand side). The main diffractions are indicated. The dark field images of the C40 $TiSi_2$ (b) and C49 $TiSi_2$ (c) are reported.

four well defined peaks at 39°, 42.5°, 43.5°, 50° attributed to C54 (311), C54 (040), C54 (022), C54 (331), and two peaks at 28.5° and 47.5°, attributed to the Si(111) and Si(220). X-ray analyses in the B–B configuration were performed on the same samples in order to evidence any eventual texturing of the film and the resulting pattern are shown in Fig. 3(a). The three sharp peaks at 38.3° (Nos. 2, 3, and 4), 41.7° (No. 2) and 44.5° (Nos. 1 and 3), not visible in the G-A configuration, can not be due to diffraction by family planes of C49 or C54 $TiSi_2$ or C40 $TaSi_2$ or Si. The origin of these peaks could be the hexagonal C40 $TiSi_2$, in agreement with former x-ray observation[9] on a similar Si/Ta/Ti system, reporting the formation of a hexagonal compound having lattice parameters $a=0.47\pm0.01$ nm and $c=0.649\pm0.001$ nm. If this is the case, the peaks at 38.3°, 41.7°, and 44.5° are due to C40 $TiSi_2$ $(2\bar{1}0)$, C40 $TiSi_2$ (003), C40 $TiSi_2$ (200), respectively. The peak at 39° (No. 4) is attributed to C54 $TiSi_2$ (131). The rocking curves of the (200) and (003) C40 planes, shown in Fig. 3(b), have full width at half maximum 0.2° and 1°, respectively. The texture of C40 $TiSi_2$ probably derives from the epitaxial growth of the latter on the C40 $TaSi_2$ layer because of the large similarity of the lattice.[9] This hypothesis should be confirmed if the C40 $TaSi_2$ results are also textured on the same directions. Unfortunately, this measurement can not be done because the $TaSi_2$ layer is too thin to give a significant signal in B–B configuration.

Therefore, our *in situ* and *ex situ* analyses indicate that a Ta layer at the interface between Ti and Si inhibits the C49 $TiSi_2$ phase formation. Then, the first sheet resistance drop in Fig. 2(a) can be attributed to the formation of the C40 $TiSi_2$ phase, while the second drop is due to the C40–C54 transition.

The transmission electron diffraction images of the partially reacted samples A and B after the formation of the intermediate phase (No. 3) are shown in Fig. 4(a). The rings in pure Si/Ti derive from the diffraction of the (131), (111) and (200) C49 $TiSi_2$ planes. In the Si/Ta/Ti system, there is a large ring containing the not resolved diffraction by three different planes: $(2\bar{1}1)$ $TaSi_2$, $(2\bar{1}\bar{1})$ C40 $TiSi_2$, and (210) C40 $TiSi_2$. The remaining ring is due to the diffraction by the (200) C40 $TiSi_2$ plane. TEM observations confirm the absence of C49 $TiSi_2$ when a Ta layer is deposited at the Si/Ti interface.

The dark field images obtained using the diffraction rings evidenced by the circles in Fig. 4(a) are shown in Figs. 4(b) and 4(c). The grains size in sample A [Fig. 4(c)] ranges between 10–100 nm and is definitely larger than in sample B [Fig. 4(b)], having grain diameters between 5–20 nm.

In a previous paper,[8] it has been reported that the C40 $TiSi_2$–C54 transition is nucleation limited and that the nucleation sites density is about an order of magnitude higher with respect to the nucleation sites density of the C49–C54 transition.[2,15] The nucleation barrier energy ΔG^* for the C40 $TiSi_2$–C54 has been reported[14] to be $\approx$0.2 eV suggesting a heterogeneous nucleation of the C54 phase at grain boundaries or at the triple grain boundaries of the C40 $TiSi_2$. The

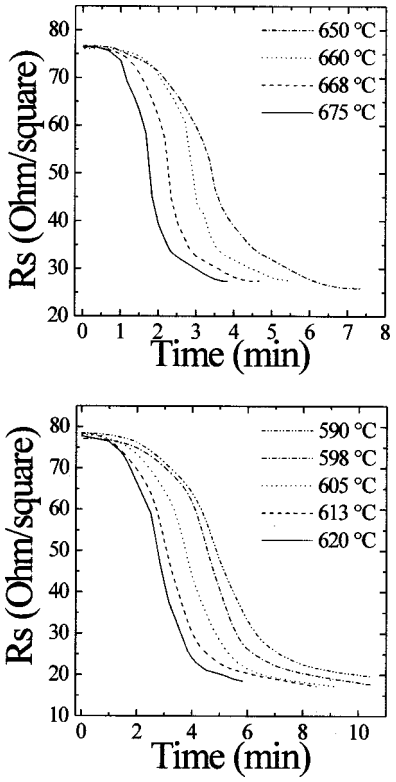

FIG. 5. *In situ* sheet resistance measurements of the C49 $TiSi_2$ (a) and of the C40 $TiSi_2$ (b) formation.

higher nucleation sites density of the C40–C54 $TiSi_2$ transition with respect to the C49–C54 can therefore be attributed to the smaller C40 grain size with respect to the C49 phase.

We have seen that each of the different $TiSi_2$ phases has a well-defined resistivity, so that the kinetics of the transformation can be derived from the sheet resistance versus time curves measured at several temperatures. In Figs. 5(a) and 5(b), the curves relative to the formation of the C49 (sample A without Ta) and C40 (sample B, 1.9×10^{15} Ta/cm^2) phases are reported. In both cases, the time to complete the transformation decreases with increasing temperature, however, lower temperature must be used in Si/Ta/Ti with respect to Si/Ti to get comparable transition times.

The activation energy E_a for the phase transformation was extracted by plotting the natural logarithmic of the time at which all the film was transformed τ, versus 1/kT (Fig. 6), where k is the Boltzmann constant and T the temperature. Based on the Arrhenius equation: $\tau=\tau_0\exp(E_a/\mathrm{kT})$ (with τ_0 constant with units of time), we obtain a linear relationship whose slope yields the effective activation energy E_a for the phase transformation. The Arrhenius plots for the three different samples are reported in Fig. 6 and it is evident that the temperature needed to obtain the C40 phase is considerably lower than that for the C49 formation.

The values of the activation energy for the formation of the first phase are summarized in Table I.

The value obtained for the Si/Ti sample is different with respect to Si/Ta/Ti cases because it refers to the formation of different phases, and it is close to the value given by Clevenger *et al.*[10] The activation energy for the C40 $TiSi_2$ formation is independent of the thickness of the Ta film.

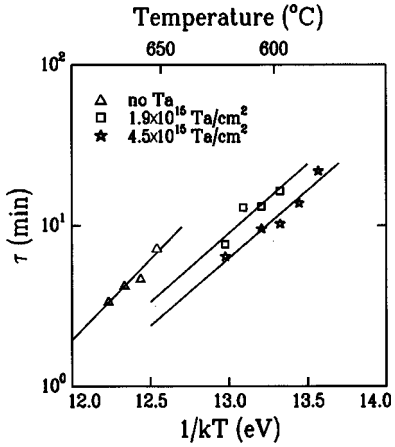

FIG. 6. Arrhenius plot of the time to form half of the C49 or the C40 $TiSi_2$ layer. The kinetic of the C40 $TiSi_2$ formation does not depend on the tantalum thickness.

The sheet resistance has been converted into fraction of reacted material and from this the rate of the C49 and C40 $TiSi_2$ has been derived. The rate of the C49 transformation has been nicely fitted by the Johnson–Mel–Avrami model using $n=3$ in agreement with a nucleation controlled transformation. The same model could not fit the rate of the C40 transformation, but the plot of the fraction of C40 formed versus the square root of time (not shown) exhibited two different slopes that suggests a diffusion controlled process. The main diffusing species is Si since it has been reported[9] that the $TaSi_2$ layer remains at the Si interface whilst a shift toward the surface is expected if Ti would be the main diffusing species. Therefore, the first slope is due to the Si diffusion through the $TaSi_2$ layer (during the initial stage of the reaction) and the final slope is due to the Si diffusion through the already formed C40 $TiSi_2$ layer. In this case, the activation energy derived from the Arrhenius plot does not have a physical meaning since it is related to different diffusion processes that can not be separated in this plot. Further experiments are needed to obtain the diffusion coefficients of Si in $TaSi_2$ and in C40 $TiSi_2$.

From the results previously shown, we can conclude that the C40 $TiSi_2$ phase growths epitaxially on the $TaSi_2$ C40 phase by solid state reaction. This epitaxial growth is promoted by the low lattice mismatch between the two phases ($\sim$1.5%),[9] while the direct epitaxial growth of the C54 on the tantalum silicide grains is strongly disadvantaged by the higher strain energy (average lattice mismatch $\sim$14%).

The sheet resistance versus time for the formation of the C54 phase at four different temperatures for samples A and B

TABLE I. Activation energies of the C49 $TiSi_2$ and C40 $TiSi_2$ formation (first transition) and for the transition of the C49 and the C40 to the C54 $TiSi_2$ phase (second transition).

Sample	Activation energy first transition	Activation energy second transition
A	1.74±0.13	5.10±0.89
B	1.98±0.61	3.78±0.84
C	1.94±0.29	3.64±0.51

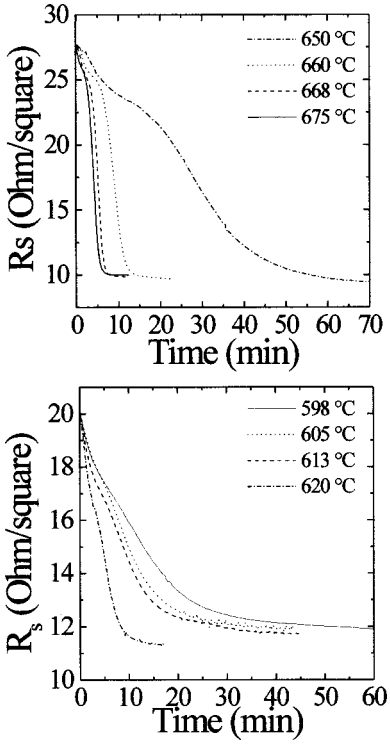

FIG. 7. *In situ* sheet resistance measurements of the C49–C54 (a) and of the C40–C54 (b) transitions.

are reported in Fig. 7(a) and 7(b), respectively. Also in this case, by increasing the annealing temperature, the transition time decreases, and, although in the Si/Ta/Ti samples the temperature used are lower than Ti/Si ones, the transition time is similar.

Following the usual procedure, the *in situ* sheet resistance data of the C49–C54 transition have been transformed into the C54 fraction by the usual series resistance model[2] and fitted (not shown) with a Johnson–Mel–Avrami equation with the exponent $n=3$ as already reported in the literature.[2,15] The same kind of data analysis has been performed for the C40 $TiSi_2$–C54 transition. In this case a reasonable fit of the data with $n=2$ can be done only in the experiments performed at the highest temperatures. In fact, as it can be observed even in Fig. 7(b), the *in situ* sheet resistance measurements are not symmetric with respect to the time to transform half of the layer. The activation energy E_a for the phase transformation was extracted, even in this case, by plotting the natural logarithmic of the time at which all the film was transformed, versus 1/kT (Fig. 6). The Arrhenius plots for the formation of the C54 phase are reported in Fig. 8 for the three samples. The activation energies for the formation of the C54 are summarized in Table I.

The activation energy of the transition from C49 to C54 is in agreement with previous works[10–12] in which the value was estimated in the range 3.5–6 eV while samples B and C have an activation energy lower than Ti/Si (Fig. 8). Of course, we observe a different value of activation energy because in sample A, the transition is from the C49 to the C54, while in the case of B and C, it is from the C40 to the C54.

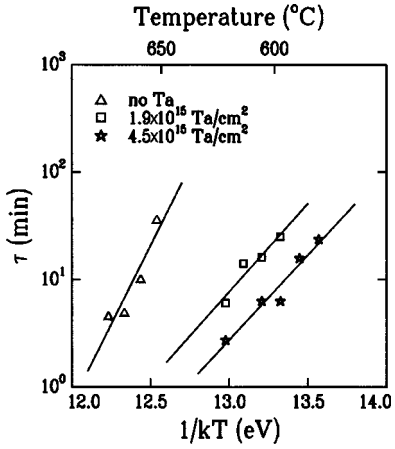

FIG. 8. Arrhenius plot of the time to transform half of the C49 or the C40 $TiSi_2$ layer in C54.

The lower value of the activation energy of the C40–C54 transition with respect to the C49–C54, one can be explained using the following arguments. From the calculations of the bulk free energy of the different $TiSi_2$ phases reported in a previous paper[13] it is known that the free energy variation in the C49–C54 transition is larger than the free energy variation of the C40–C54 one. But, at the same time, the interface energy between the C40 and the C54 is much lower than the interface energy between the C49 and the C54. In fact, the C40 has a structure very similar to the C54 structure and on several planes, it is possible to have a perfect mismatch between the two phases. The combination of these two behaviors produces a lower nucleation barrier energy ΔG^* (about 0.2 eV)[14] with respect to the nucleation barrier energy of the C49–C54 transition (about 0.4 eV).[15] Furthermore, also the growth rate of the C54 is much faster[14] starting from the C40. In fact, from an microscopic point of view, to go from the C40 to the C54 structure only a few atom displacements are needed, while, in the case of the C49–C54 transition, all the chemical bonding should be broken. The final result is that a lower total energy is necessary to form the C54 starting from the C40 phase.

IV. CONCLUSION

From our results, it is clear that a phase (the C40 $TiSi_2$) is formed when a thin tantalum layer is deposited at the Si/Ti interface. The proposed reaction path is the following: C40 $TaSi_2$ is the first phase formed at the silicon interface. This phase is the seed for the successive growth of C40 $TiSi_2$ that suppress the formation of the C49 phase because of its faster kinetics. Finally, the C40–C54 transformation occurs by nucleation and growth of the stable phase. The reaction kinetic of C40 $TiSi_2$ formation and that of the C40–C54 $TiSi_2$ transition has been detailed studied and compared with those of C49 $TiSi_2$ and C49–C54 $TiSi_2$. The activation energy for the C40 $TiSi_2$ formation ($\approx$1.9 eV) does not depend on the tantalum thickness as well as the activation energy of the C54 formation starting from the C40 $TiSi_2$. It has been demonstrated that the rate of C40 formation is controlled by diffusion of Si. The C40–C54 $TiSi_2$ transition is nucleation con-

trolled as the C49–C54 $TiSi_2$ but it occurs at a lower temperature because of both a higher density of nucleation sites and lower activation energy.

ACKNOWLEDGMENTS

This work was partially supported by CNR Grant Nos. CT88.00042.PF30 and 97.01355 PS48. The authors would like to thank S. Pannitteri (CNR-IMETEM) for TEM analysis.

[1] R. Beyers and R. Sinclair, J. Appl. Phys. **57**, 5240 (1985).
[2] S. Privitera, F. La Via, M. G. Grimaldi, and E. Rimini, Appl. Phys. Lett. **73**, 3863 (1998).
[3] R. W. Mann, G. L. Miles, T. A. Knotts, D. W. Rakowski, L. A. Clevenger, J. M. E. Harper, F. M. D'Heurle, and C. Cabral Jr. Appl. Phys. Lett. **67**, 3729 (1995).
[4] C. Cabral, L. A. Clevenger, J. M. E. Harper, F. M. d'Heurle, R. Roy, C. Lavoie, and K. Saenger, Appl. Phys. Lett. **71**, 3531 (1997).
[5] A. Moroux, S. L. Zhang, and C. S. Peterson, Phys. Rev. B **56**, 10 614 (1997).
[6] J. A. Kittl, M. A. Gribelyuk, and S. B. Samavedam, Appl. Phys. Lett. **73**, 900 (1998).
[7] A. Moroux, T. Epicier, S. L. Zhang, and P. Pinard, Phys. Rev. B **60**, 9165 (1999).
[8] F. La Via, F. Mammoliti, M. G. Grimaldi, S. Quilici, and F. Meinardi, Microelectron. Eng. **55**, 123 (2001).
[9] F. La Via, F. Mammoliti, G. Corallo, M. G. Grimaldi, L. Miglio, and D. Migas, Appl. Phys. Lett. **78**, 1864 (2001).
[10] L. A. Clavenger, R. W. Mann, R. A. Roy, K. L. Saenger, C. Cabral Jr., and J. Picirillo, J. Appl. Phys. **76**, 7874 (1994).
[11] E. G. Colgan, L. A. Clevenger, and C. Cabral, Appl. Phys. Lett. **65**, 2009 (1994).
[12] Z. Ma and H. Allen, Phys. Rev. B **49**, 13 501 (1994).
[13] F. Bonoli, M. Iannuzzi, L. Miglio, and V. Meregalli, Appl. Phys. Lett. **73**, 1964 (1998).
[14] F. La Via, S. Privitera, F. Mammoliti, and M. G. Grimaldi (unpublished).
[15] S. Privitera, F. La Via, C. Spinella, S. Quilici, A. Borghesi, F. Meinardi, M. G. Grimaldi, and E. Rimini, J. Appl. Phys. **88**, 7013 (2000).